

Conditional ablation of Notch signaling in pancreatic development

Hassan Nakhai^{1,*}, Jens T. Siveke^{1,*}, Bettina Klein², Lidia Mendoza-Torres¹, Pawel K. Mazur¹, Hana Algül¹, Freddy Radtke³, Lothar Strobl⁴, Ursula Zimmer-Strobl⁴ and Roland M. Schmid^{1,†}

The role of the Notch signaling members *Notch1*, *Notch2* and *Rbpj* in exocrine pancreatic development is not well defined. We therefore analyzed conditional pancreas-specific *Rbpj* and combined *Notch1/Notch2* knockout mice using *Ptf1a^{+Cre(ex1)}* mice crossed with floxed *Rbpj* or *Notch1/Notch2* mice. Mice were analyzed at different embryonic stages for pancreatic exocrine and endocrine development. The absence of *Rbpj* in pancreatic progenitor cells impaired exocrine pancreas development up to embryonic day 18.5 and led to premature differentiation of pancreatic progenitors into endocrine cells. In *Rbpj*-deficient pancreata, amylase-expressing acini and islets formed during late embryonic and postnatal development, suggesting an essential role of *Rbpj* in early but not late development. Contrary to this severe phenotype, the concomitant inactivation of *Notch1* and *Notch2* only moderately disturbed the proliferation of pancreatic epithelial cells during early embryonic development, and did not inhibit pancreatic development. Our results show that, in contrast to *Rbpj*, *Notch1* and *Notch2* are not essential for pancreatogenesis. These data favor a Notch-independent role of *Rbpj* in the development of the exocrine pancreas. Furthermore, our findings suggest that in late stages of pancreatic development exocrine cell differentiation and maintenance are independent of *Rbpj*.

KEY WORDS: Notch, *Rbpj*, Conditional knockout mice, Pancreas, Development

INTRODUCTION

The Notch signaling pathway is a key regulator of developmental processes during organogenesis. Loss-of-function studies have proposed that Notch signaling regulates self-renewal leading to depletion of pancreatic progenitor cells and accelerated differentiation of endocrine cells (Apelqvist et al., 1999; Fujikura et al., 2006; Fujikura et al., 2007; Jensen et al., 2000). While these studies have provided evidence for an important role of Notch signaling in endocrine development, the dependence of the exocrine compartment on specific Notch signaling members is not well understood. Recently, RBPJ κ , the transcriptional mediator of Notch signaling, was found to be a binding partner of PTF1A in the PTF1 complex, suggesting a Notch-independent function during pancreatic development (Beres et al., 2006; Masui et al., 2007). Moreover, because of the existence of multiple receptors, ligands and target genes, and because of the embryonic lethality of mice null for Notch signaling components, the precise role of individual Notch signaling components in early and late pancreatic organogenesis is not well defined. During pancreatic organogenesis, *Notch1* and *Notch2* expression has been described in the pancreatic epithelium, whereas *Notch3* and *Notch4* are expressed in mesenchymal and endothelial cells (Lammert et al., 2000).

In order to clarify the role of the epithelially expressed receptors *Notch1* and *Notch2* versus the abrogation of RBPJ κ signaling, we analyzed conditional *Notch1/Notch2* double-knockout and *Rbpj* knockout mice by using *Ptf1a^{+Cre(ex1)}* mice for targeting pancreatic progenitor and exocrine cells.

MATERIALS AND METHODS

Generation of *Rbpj^{fl/fl}* mice

In order to generate a conditional gene replacement vector for *Rbpj*, several genomic fragments of *Rbpj* were isolated from a λ -DASHII phage library (Stratagene) and subcloned into pBluescript SK+ (Stratagene). A neomycin resistance cassette, flanked by two *loxP* sites, was inserted into intron 7, and a single *loxP* site was integrated into intron 5. A herpes simplex virus thymidine kinase (HSV-tk) cassette was cloned at the 5' end of the gene-targeting construct (Fig. 1A). The *Not1*-linearized vector was transfected into murine 129/SvJ ES cells, where it recombined with the host genome. The homologous recombination event occurred at a frequency of 1:602 and was verified by PCR and Southern blot analysis. The floxed *neo*-resistance cassette was removed by transient transfection of a vector expressing the Cre-recombinase. Blastocyst injection and germline transmission of the mutant allele were done as described previously (Tanigaki et al., 2002). Genotyping of mice was performed on DNA isolated from tail biopsies using a PCR kit (Qiagen). For the detection of floxed (0.55 kb fragment) and wild-type (0.5 kb) alleles of *Rbpj*, PCR amplification (1 minute at 94°C, 30 seconds at 58°C and 30 seconds at 72°C, for 40 cycles) was carried out using primers 5'-AGT TTA GGC TTT CCA AAA GGC-3' (forward) and 5'-GTA TTG CTA AGA ACT TGT TGC-3' (reverse). All mice were housed in pathogen-free conditions. All mouse protocols were approved by the Centre of Animals Research, the Faculty of Medicine, Technical University of Munich.

X-gal staining

β -gal activity was determined on whole-mount preparations as described previously (Kawaguchi et al., 2002).

BrdU labeling

In vivo pulse labeling with 5-bromo-2-deoxyuridine (BrdU) was used to mark newly synthesized DNA. BrdU (20 mmol/l, 5 ml/kg body weight) was injected intraperitoneally into pregnant mice 2 hours before sacrifice.

Histology and immunohistology

Dissected tissues were fixed in ice-cold 4% paraformaldehyde, paraffin-embedded and cut into 2-3 μ m sections. Immunohistochemistry was performed using the following primary antibodies: rabbit anti-PTF1A (1:500, kind gift from Raymond J. Macdonald, University of Texas, USA); rabbit anti-PDX1 (1:10,000, kind gift from C. V. Wright, Vanderbilt University Medical

¹Department of Internal Medicine, Technical University of Munich, Ismaninger Strasse 22, 81675 Munich, Germany. ²Institute of Immunology, Friedrich-Loeffler Institut, Paul-Ehrlich Strasse 28, 72076 Tuebingen, Germany. ³ISREC, Chemin des Boveresses 155, 1066 Epalinges, Switzerland. ⁴GSF-National Research Center for Environment and Health, Institute for Clinical Molecular Biology and Tumor Genetics, Marchioninistrasse 25, 81377 Munich, Germany.

*These authors contributed equally to this work

†Author for correspondence (e-mail: roland.schmid@lrz.tum.de)

Center, Nashville, USA); guinea pig anti-insulin (1:1000, Linco); rabbit anti-glucagon (1:1000, Linco); guinea pig anti-glucagon (1:500, Linco); rabbit anti- β -galactosidase (1:500, ICN); rabbit anti-somatostatin (1:1000, ICN); rabbit anti-pancreatic polypeptide (1:500, BioTrend); rabbit anti-amylase (1:1000, Sigma) rabbit anti-phosphohistone H3 (1:500, Upstate); rabbit anti-carboxypeptidase A (1:500, BioTrend); mouse anti-CK19 [1:500, Developmental Studies Hybridoma Bank (DSHB), University of Iowa]; rabbit anti-HES1 (1:100, kind gift from T. Sudo, Toray Industries, Tokyo, Japan); rabbit anti-cyclin B1 (1:500, Millipore); rat anti-BrdU (1:250, Serotec); mouse anti-Neurogenin (1:500, DSHB). For immunoperoxidase detection, Vectastain ABC kit (Vector Labs) was used according to the manufacturer's instructions. For double immunofluorescence staining, the primary antibodies were followed by incubation with secondary antibodies conjugated with fluorescent Alexa 488 or Alex 568 (Molecular Probes). Sections were mounted with Vectashield mounting medium (Vector Laboratories) and examined using an Axiovert 200M (Zeiss) fluorescent inverse microscope equipped with the Axiovision version 4.4 software (Zeiss). The number of islets was calculated, with the definition of an islet being a group of β cells surrounded by α cells. For morphometric analyses, the pancreatic buds were immunostained with anti-PDX1 and analyzed using the AxioVision Image analysis software (Zeiss). To calculate the number of PHH3- and neurogenin 3-positive cells, whole pancreatic buds from three control and three knockout embryos were cut into 3 μ m serial sections. Every fifth section was stained and the number of PHH3⁺, neurogenin 3⁺ and insulin⁺ cells were counted and calculated relative to the whole area of PDX1⁺ pancreatic epithelium in every section.

Laser capture microscopy

Acini and pancreatic buds were dissected from 5- to 6- μ m sections using a Leica and P.A.L.M microlaser system, respectively. Cells were incubated overnight at 37°C in 20 μ l of TE buffer [1 mM EDTA, 20 mM Tris (pH 8)] containing 0.5 mg/ml proteinase K, after which the proteinase K was heat inactivated by incubation at 95°C for 15 minutes. For detection of the floxed (0.33 kb) and deleted (0.30 kb) alleles of *Notch1*, PCR amplification (94°C for 20 seconds, 55°C for 30 seconds, and 72°C for 30 seconds, for 40 cycles) was performed using primers P1 (5'-AAC TGA GGC CTA GAG CCT TGA AG-3'), P2 (5'-GTG GTC CAG GGT GTG AGT GTT C-3') and P3 (5'-ACC TGT TCG CAG GCA TCT CCA G-3'). Floxed (0.29 kb) and deleted (0.37 kb) alleles of *Notch2* were detected using primers P4 (5'-GGA GAA GCA GAG ATG AGC AGA TGG-3'), P5 (5'-CAC ATG TGC GTG CGT GTG CAT G-3'), P6 (5'-CAG AGA TGA GCA GAT GGG CAT A-3') and P7 (5'-GAG GCC AGA GGA CGA CTC TGT-3'). For *Rbpj*, a 2-kb (floxed) and a 0.75-kb (deleted) fragment were obtained using primers P8 (5'-TAT TGC TAA GAG CTT GTT GC-3') and P9 (5'-ACT GAG TGT GTA TCT TAA GC-3').

Western blot analysis

Whole-cell lysates were prepared and western blots were performed as previously described (Siveke et al., 2007).

RESULTS

Generation of pancreas-specific *Rbpj* and *Notch1/Notch2* knockout mice

Ptf1a^{+/*Cre(ex1)*} mice were generated using a knock-in approach replacing exon 1 with Cre recombinase (Nakhai et al., 2007). For analysis of Cre recombinase expression, *Ptf1a*^{+/*Cre(ex1)*} mice were crossed to *Rosa26R*^{lacZ} (*R26R*) reporter mice (Soriano, 1999). In pancreata of newborn mice, Cre-induced recombination measured by X-gal staining occurred as expected from previous studies (Kawaguchi et al., 2002) (data not shown). To abrogate Notch receptor signaling, an approach generating either *Rbpj* or *Notch1/Notch2* double-knockout mice was chosen. For simplicity, *Ptf1a*^{+/*Cre(ex1)*};*Rbpj*^{fl/fl} will be termed *RbpjKO* and *Ptf1a*^{+/*Cre(ex1)*};*Notch1*^{fl/fl};*Notch2*^{fl/fl} will be termed *Notch1/2KO* mice; heterozygote littermates and littermates not expressing Cre recombinase will be termed *Rbpj*^{+/-}, *Notch1/2*^{+/-} and *WT* mice, respectively.

To generate pancreas-specific, *Rbpj*-knockout mice, *loxP* sites were inserted flanking exons 6 and 7 of *Rbpj* in embryonic stem cells (ES) by homologous recombination (Fig. 1A). ES cell clones with a floxed (*f*) *Rbpj* locus were used to generate chimeric mice. The mutant mouse line (*Rbpj*^{+/*f*}) was established through germline transmission. Cre-recombinase-mediated deletion of exon 6 and 7 of *Rbpj* resulted in a mutant RBP-Jk protein lacking a functional DNA-binding domain. By crossing *Rbpj*^{fl/fl} mice with a Nestin-Cre deleter line, we were not able to obtain *Rbpj*-deficient newborns, and this provides strong evidence for a functionally null *Rbpj* transcript after Cre-induced recombination (data not shown). For pancreas-specific targeting, we next crossed *Rbpj*^{fl/fl} mice with *Ptf1a*^{+/*Cre(ex1)*} mice. *Ptf1a*^{+/*Cre(ex1)*} mediated deletion of the *Rbpj* gene was verified by Southern blot analysis with DNA from different tissues of newborn *Ptf1a*^{+/*Cre(ex1)*};*Rbpj*^{+/*f*} offspring (Fig. 1B). For conditional knockout of *Notch1* and *Notch2*, previously described *Notch1*^{fl/fl} and *Notch2*^{fl/fl} mice were used (Radtko et al., 1999; Schouwey et al., 2006). As we did not find qualitative defects in pancreatic organogenesis, nor major abnormalities in the unstimulated adult pancreata of conditional *Notch1*, *Notch2* or combined *Notch1/Notch2* knockout mice over an observation period of 18 months (Siveke et al., 2008) (data not shown), combined *Notch1/2KO* were chosen for the analysis of pancreatic development. In *Notch1* and *Notch2* single receptor knockouts, as well as in double-knockout pancreata, *Notch1* and *Notch2* protein and transcripts were decreased to less than 10%, as analyzed by western blot and RT-PCR (data not shown). Both, *Rbpj* and *Notch1/Notch2* knockout lines were tested for the possibility of mosaic Cre-induced recombination using *Rosa26R* reporter mice as a surrogate for recombination-induced deletion of *Rbpj* or *Notch1/Notch2*, respectively. Using X-gal staining, we did not observe X-gal-negative exocrine cells in adult pancreata (Fig. 1G-I). Regarding recombination in the endocrine compartment, we found approximately 50% of endocrine cells to be X-gal positive, a recombination pattern that was very similar to that observed in *Ptf1a*^{+/*Cre(ex1)*};*Rosa26R*^{lacZ} pancreata (Fig. 5M-U).

Although heterozygous *Rbpj*^{+/-} and homozygous *Notch1KO*, *Notch2KO* and *Notch1/2KO* mice showed no gross abnormalities and developed normally, *RbpjKO* mice survived only until 4-5 days postpartum. Although moderate signs of growth retardation were observable at birth (Fig. 1C), the early death was caused by insufficient postnatal growth with impaired milk digestion. We were able to raise some *RbpjKO* mice to adulthood by feeding them with pancreatic enzyme-enriched animal food (data not shown). Examination of the *RbpjKO*;*R26R* mice at day 1 postpartum (dpp) revealed a small and severely altered pancreas (Fig. 1F,I). In the duodenal part of the mutant pancreas, weakly branched ducts were observable (Fig. 1F, arrowhead), whereas the splenic part of the pancreas showed no branching (Fig. 1F, arrows). Histological examination demonstrated a lack of acinar tissue with large duct-like structures being present in the splenic and duodenal portion of the pancreas (Fig. 1I, blue). Interestingly, *Notch1/2KO* mice did not reveal striking abnormalities in pancreatic tissue organization or cell lineage distribution, suggesting a non-essential role for *Notch1* and *Notch2* during pancreatic development. However, the mutant pancreas was noted to be slightly smaller than that of wild type when analyzed at 1 dpp (Fig. 1E,H). To further clarify the role of ablated Notch signaling, early stages of pancreatogenesis were investigated.

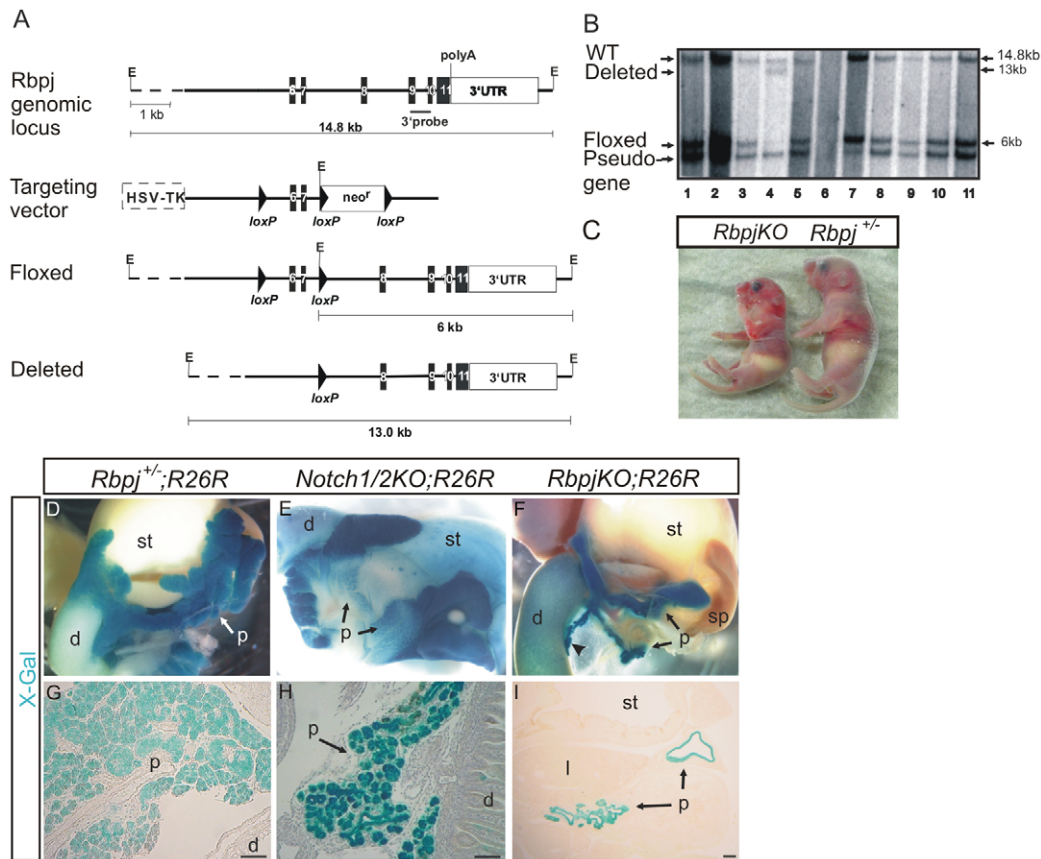


Fig. 1. Pancreas-specific *Rbpj* and *Notch1/2KO* mice. (A) Strategy for targeting the *Rbpj* locus to generate *Rbpj*^{+/±} mice. The *loxP* sequences (arrowheads), exons (filled boxes), length of diagnostic restriction fragments and location of a 3'-probe (bar) used for Southern blotting are shown. *EcoRI* restriction enzyme sites (E) are indicated. (B) Southern blot analysis of Cre-mediated deletion in the following organs of an *Ptf1a*^{+/Cre(ex1)};*Rbpj*^{+/±} mouse: thymus (lane 1), spleen (2), liver (3), pancreas (4), kidney (5), head (6), lung (7), salivary gland (8), stomach (9), duodenum (10), and coecum (11). The positions and sizes of the fragments derived from the wild-type (WT), deleted, *floxed* and pseudogene alleles are indicated. (C) Newborn *Rbpj*KO mice show increasing signs of growth retardation and die 4-5 days postpartum. (D-I) Macroscopic (D-F) and microscopic (G-I) X-gal staining analysis of intestinal tracts from newborn mice show X-gal⁺ pancreata (blue) from *Rbpj*KO;R26R, *Notch1/2KO*;R26R and *Rbpj*^{+/±};R26R pups. Arrowhead in F indicates weakly branched ducts in pancreatic rudiment. *neo^r*, neomycin-resistance gene; HSV-tk, herpes simplex virus thymidine kinase gene; d, duodenum; l, liver; p, pancreas; sp, spleen; st, stomach. Scale bar: 100 μm.

Early pancreatic development in *Rbpj*- and *Notch1/Notch2*-deficient pancreata

To analyze pancreatic development at defined stages of pancreatic organogenesis, we investigated pancreatic bud development at embryonic day 10 (E10) to E13.5 by immunohistochemistry and X-gal staining. The pancreatic buds of E13.5 *Rbpj*^{+/±};R26R and *Notch1/2KO*;R26R embryos displayed the typical branching of the pancreatic epithelium. The *Notch1/2KO* buds appeared smaller and less branched than in control littermates (Fig. 2A,B,D). By contrast, *Rbpj*KO;R26R embryos revealed a significantly reduced epithelial mass with weakly branched structures in both buds (Fig. 2C,D), suggesting that *Rbpj* is essential for the expansion of the pancreatic epithelium.

As *Hes1* is one of the target genes of *Rbpj*-dependent Notch signaling activation, we analyzed HES1 expression at E12.5. At this stage, HES1 protein was broadly detected within the nuclei of PDX1⁺ epithelial cells, as well as in PDX1⁻ mesenchymal elements (Fig. 2E). Compared with *Rbpj*^{+/±};R26R littermate controls, *Rbpj*KO and *Notch1/2KO* mice showed reduced, although not absent, HES1 expression in PDX1⁺ pancreatic cells, suggesting efficient ablation of Notch signaling (Fig. 2E-G). As the premature differentiation of

pancreatic progenitor to endocrine cells has been suggested previously as a possible cause for the reduction of pancreatic epithelium in *Rbpj*-deficient buds (Fujikura et al., 2006), pancreatic sections at E11.5 were stained for X-gal and glucagon expression. In *Rbpj*^{+/±};R26R embryos, glucagon-expressing cells formed small clusters peripheral to and dispersed within the dorsal bud (Fig. 2H, brown). Similar to *Rbpj*^{+/±};R26R mice, *Notch1/2KO* mice showed no increased number of glucagon-positive cells (Fig. 2I, brown). By contrast, we observed an increased number of glucagon-positive cells in *Rbpj*KO;R26R embryos at this time point, consistent with the premature differentiation of pancreatic progenitors to endocrine cells. These cells were found within and peripheral from the ventral and dorsal buds (Fig. 2J, brown).

As expression of the transcription factor neurogenin 3 (*Ngn3*) is a prerequisite for endocrine lineage development, E13.5 pancreata were analyzed for expression of NGN3. Consistent with previous results, we found decreased numbers of NGN3⁺ cells in *Rbpj*KO mice at this stage (Fig. 2M,N), when compared with *Rbpj*^{+/±};R26R embryos (Fig. 2K,N), suggesting an early commitment of these cells to endocrine cell lineages. We also found more insulin⁺ β cells per PDX1⁺ area in *Rbpj*KO pancreata (Fig. 2Q,R). Regarding the differentiation of

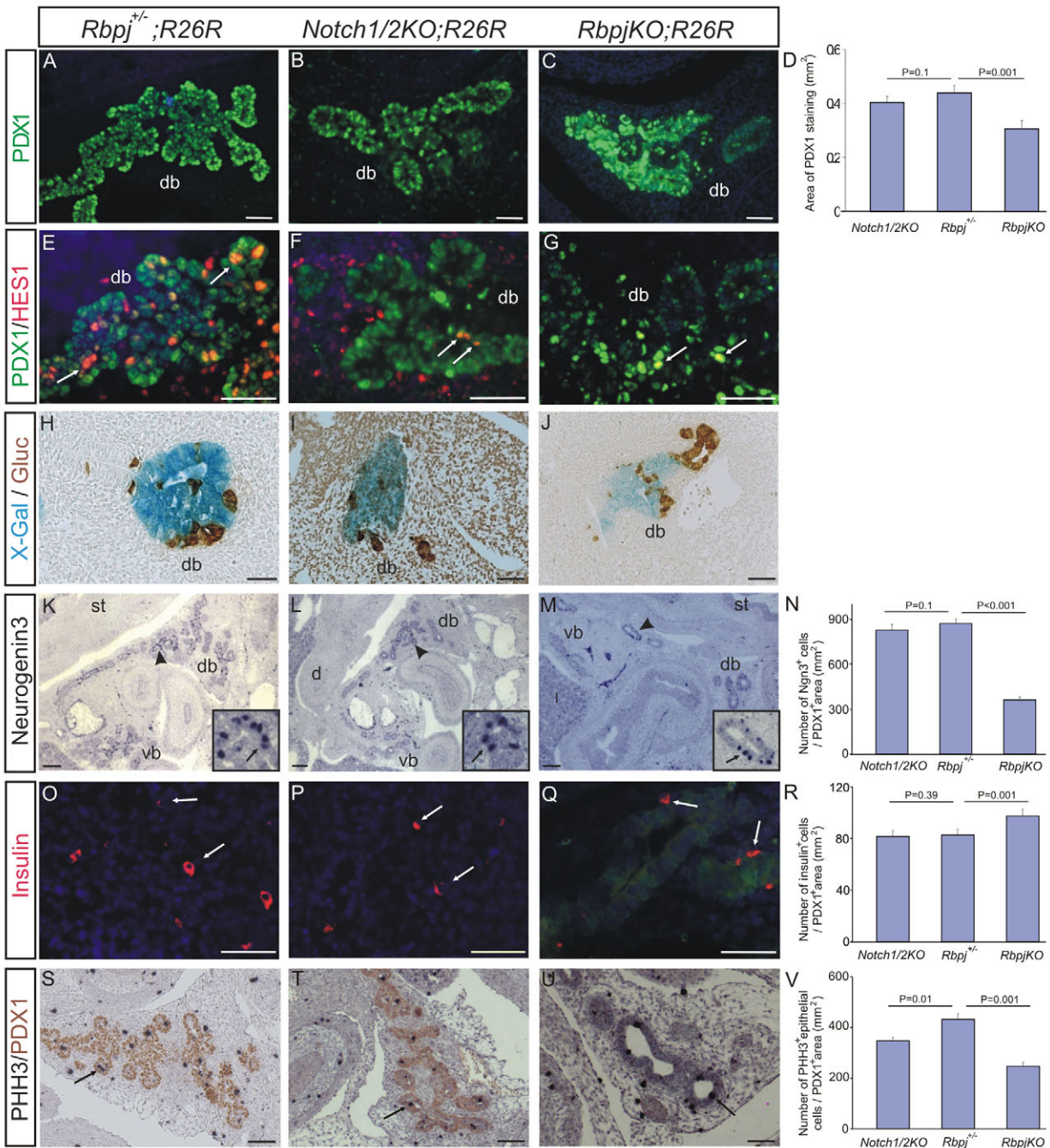


Fig. 2. Analysis of early pancreatic development in mutant embryos. (A-C) Pancreatic development of the respective mutant embryos at E13.5 as determined by PDX1 immunofluorescence (green). (E-G) Immunofluorescence for PDX1 (green) and HES1 (red) in pancreatic dorsal buds of mutant embryos at E12.5. (H-J) Double staining of pancreatic dorsal buds of mutant embryos for X-gal (blue) and glucagon (brown) at E11.5. (K-M) Nuclear expression of NGN3 in E13.5 mutant pancreata by immunohistochemistry. Arrowheads mark the areas in insets (enlarged 4 \times). Arrows in insets mark NGN3⁺ cells (black). (O-Q) Insulin expression in mutant pancreata at E13.5 by immunofluorescence (red, arrows). (S-U) Double-immunostaining for phospho-histone H3 (PHH3, black, arrows) and PDX1 (brown) at E13.5. (D,N,R,V) Quantification of the number of NGN3⁺, Insulin⁺ and PHH3⁺ cells, and size of area of PDX1⁺ cells, in buds of E13.5 *Rbpj^{+/-};R26R*, *Notch1/2KO;R26R* and *RbpjKO;R26R* embryos. Histograms show the mean size \pm s.d. for ventral and dorsal buds of three embryos each. Nuclei were counterstained with DAPI. Gluc, glucagon; vb, ventral bud; db, dorsal bud. Scale bar: 50 μ m.

endocrine cells in *Notch1/Notch2*-deficient pancreata, no significant reduction of NGN3⁺ cells (Fig. 2L,N) and no related β cell increase were notable at E13.5 (Fig. 2P,R). The reduced branching and epithelial mass in the *Notch1/2KO* and *RbpjKO* embryos was accompanied by a decrease in the number of proliferating cells in pancreatic epithelium,

as detected by phospho-histone H3 (PHH3) and PDX1 double-immunostaining (Fig. 2S-U). While the relative number of the PHH3⁺ cells to PDX1⁺ cell area in *Notch1/2KO* buds was reduced by 25% in comparison with control mice (*Rbpj^{+/-};R26R*; Fig. 2S,T,V), the relative number in *RbpjKO* buds was decreased to 40% (Fig. 2U,V).

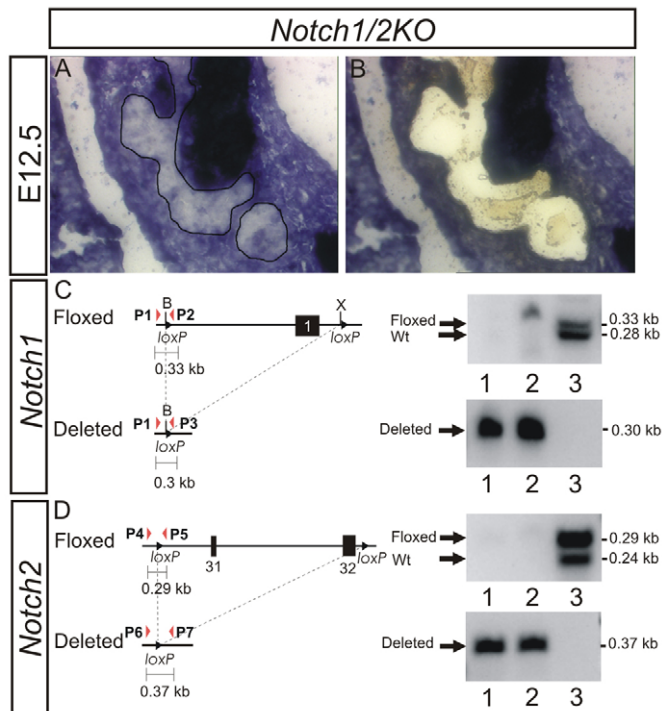


Fig. 3. Early Cre-induced recombination of *Notch1* and *Notch2* alleles in the pancreatic epithelium. (A,B) Detection of early α cells in the dorsal bud by immunostaining for glucagon at E12.5. (A) Microdissection of pancreatic epithelial cells. (B) Note that glucagon⁺ cells (dark) are not dissected. (C,D) Schematic maps of the floxed *Notch1* (C) and *Notch2* (D) locus before and after Cre-induced recombination. The position and polarity of the primers used for amplification are represented by P1, P2 and P3 for *Notch1*, and P4, P5, P6 and P7 for *Notch2* (red arrowheads). DNA was isolated from pancreatic epithelial cells of two *Notch1/2KO* embryos (lane 1 and lane 2). As a control, DNA from heterozygous *Notch1/2^{fl/fl}* mice was used (lane 3).

In contrast to the severe defects in pancreatic development observed in *RbpjKO* embryos, *Notch1/2KO* embryos showed only a marginal loss of the pancreatic mass, without defects in the development of the exocrine and endocrine compartments. One obvious explanation would be low expression, or inefficient recombination activity, of Cre recombinase during early pancreatic development, and, consequently, an inefficient inactivation of both *Notch1* and *Notch2* alleles. To determine the efficiency of Cre recombinase activity, we analyzed the recombination of the floxed *Notch1* and *Notch2* alleles by PCR analysis of microdissected epithelial cells of pancreatic buds from *Notch1/2KO* embryos at E12.5. The microdissection of early glucagon⁺ cells not expressing *Ptf1a* was avoided by immunostaining the embryonic sections for glucagon. The epithelial cells from stained sections were isolated using a P.A.L.M. Microdissection system (Fig. 3A,B). The PCR was performed with DNA from two knockout embryos using specific primers for floxed and deleted *Notch1* and *Notch2* alleles, with DNA from heterozygous *Notch1/2^{fl/fl}* embryos serving as a control for floxed and recombined alleles. For the detection of recombined DNA events, 4000 cells were used for each PCR reaction with a determined sensitivity to detect recombined alleles from DNA of about 200 cells. As shown in Fig. 3C,D, we could not detect any

floxed *Notch1* and *Notch2* fragments in the DNA of double-knockout epithelial cells. Thus, *Notch1* and *Notch2* alleles were deleted in more than 95% of epithelial cells of *Notch1/2KO* pancreatic buds.

Appearance of acinar cells during late embryonic development in *Rbpj*-deficient pancreas

Exocrine cell differentiation in *Rbpj^{+/-}* embryos was similar to that of *Rbpj^{WT}* and *Notch1/2^{WT}* embryos, suggesting that heterozygosity for *Rbpj* and/or *Ptf1a* has no profound effect on exocrine lineage development. At E14.5, well-defined exocrine acini were observable in all of the littermate controls (Fig. 4A). However, in *RbpjKO* embryos neither amylase nor carboxypeptidase A expression was detectable at E14.5 (Fig. 4C, data not shown). In contrast to this, *Notch1/2KO* pancreata revealed amylase⁺ cells, although the acinar compartment appeared smaller than in littermate controls (Fig. 4B). At E18.5, the exocrine pancreas showed no morphological differences in *Notch1/2KO*, when compared to control littermates (Fig. 4D,E). In *RbpjKO* at this stage, we surprisingly detected a few amylase⁺ acini in the duodenal part and amylase⁺ duct-like structures in the splenic portion of the rudimentary pancreas (Fig. 4F,J). These splenic amylase⁺ duct-like structures contained amylase⁺ cells (Fig. 4K, arrows), whereas most duodenal duct-like structures did not express amylase (Fig. 4L, arrow). In *RbpjKO* pups, the cells of both splenic and duodenal duct-like structures showed positive staining with CK19, a marker of differentiated ductal cells (Fig. 4I, black). These cells were also positive for X-gal staining, suggesting that all of them derived from *Rbpj*-deficient cells (Fig. 4I, arrows). In *Notch1/2KO* mice, ductal cells were CK19⁺ and similar in appearance to in control littermates (Fig. 4G,H, arrows).

In *RbpjKO* mice at E18.5, co-immunostaining for PDX1 and amylase showed that the majority of amylase⁺ cells were also PDX1⁺, and were mitotically active, as determined by BrdU labeling (Fig. 4M,N). Because a functional PTF1 complex is required for the expression of acinar genes, such as amylase, we determined the expression of PTF1A in *RbpjKO* pancreata. Here, we detected PTF1A⁺ cells surrounded by stromal cells outside the main duct and in the duodenal part of the rudimentary pancreas (Fig. 4O, arrows). To determine whether the *Rbpj* gene was actually deleted in amylase-expressing cells in the mutant pancreas, pancreatic sections from *RbpjKO* newborns were co-stained for X-gal and amylase, demonstrating the Cre-induced recombination of amylase⁺ cells (Fig. 4P). In addition, PCR analysis of DNA isolated from amylase⁺ cells by microdissection confirmed that the *Rbpj* gene was deleted in acinar cells from *RbpjKO* newborns (Fig. 4Q).

Endocrine cell development in *Rbpj*- and *Notch1/Notch2*-deficient pancreas

Most mature endocrine cells appeared after E14 in both *Notch1/2KO* and *RbpjKO* embryos, similar to in littermate controls. At E18.5, we could detect all endocrine cell lines, glucagon-producing α cells, insulin-containing β cells, somatostatin⁺ δ cells, and pancreatic polypeptide⁺ (PP) cells in both *Notch1/2KO* and *Rbpj^{+/-}* embryos. In *RbpjKO* mice, these cells were detectable in the rudimentary pancreas within the tubular duct wall and in the protruding formations of the pancreatic tubule (Fig. 5A-L).

At E18.5, most endocrine cells of the *Rbpj^{+/-}* control embryos aggregated with α cells starting to organize around core structures of β cells (Fig. 5P, arrowhead). Similar to control embryos, endocrine cells in both *Notch1/2KO* and *RbpjKO* embryos also started to aggregate; however, the number of formed islets was

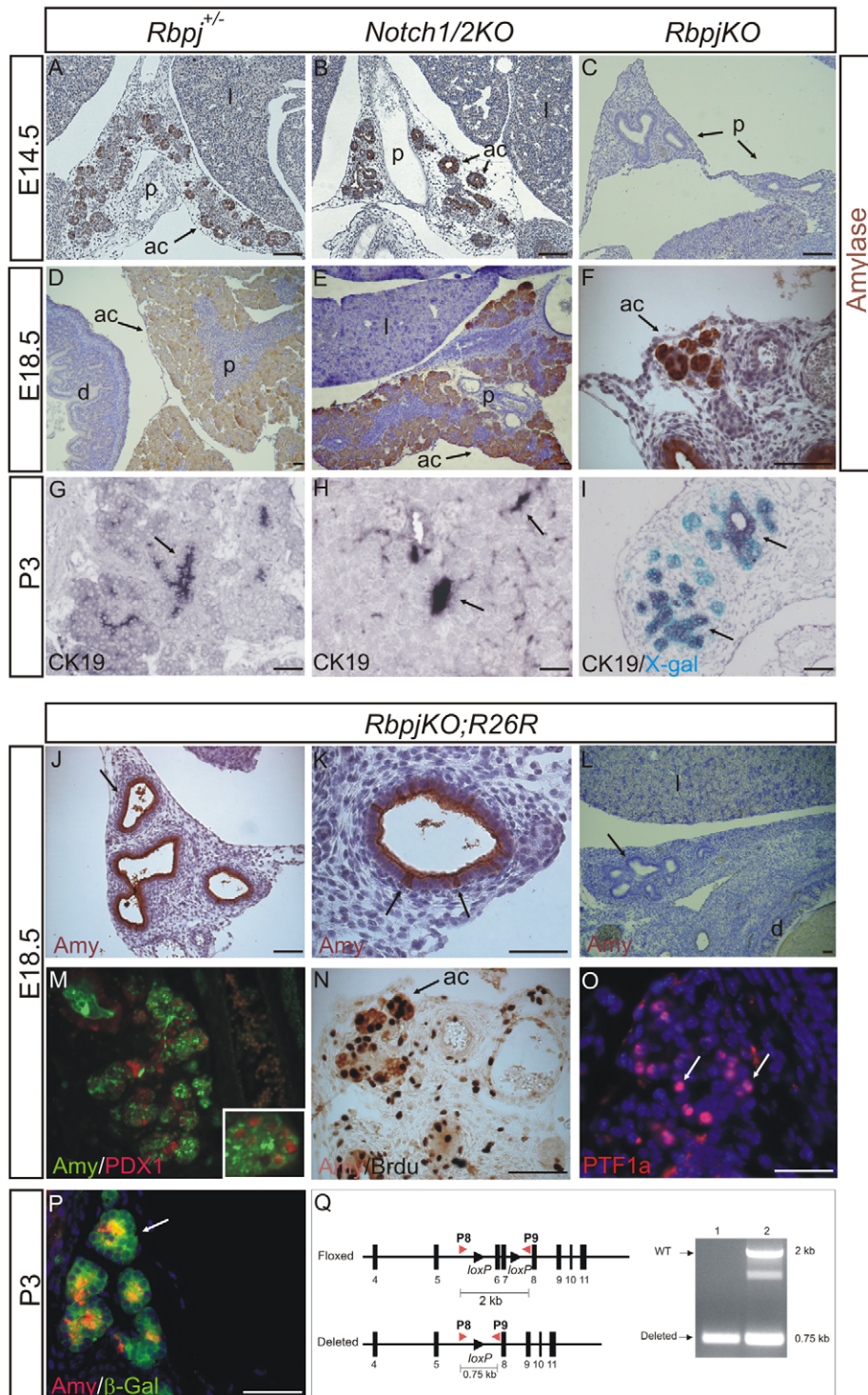


Fig. 4. Appearance of acinar cells in late stage of embryonic development of *RbpjKO* embryos. (A-F) Analysis of amylase expression at E14.5 (A-C) and E18.5 (D-F) in mutant pancreata. (G-I) Immunostaining of mutant pancreata with an antibody against the ductal marker CK19 (black, arrows) at day 3 postpartum (P3). (I) CK19 and X-gal (blue) co-staining of *RbpjKO* pancreas at P3. (J-L) Amylase staining (brown) of duct-like structures of *RbpjKO* pancreas at E18.5. In contrast to ventral bud (L), the most of dorsal duct-like structures are positive for amylase (J,K). (M-O) Amylase⁺ cells (green) from *RbpjKO* embryos express PDX1 (M, red) and PTF1A (O, red), detected by immunofluorescence, and are proliferating as determined by cytoplasmic amylase (brown) and nuclear BrdU (black) staining (N, arrow). Inset in M represents a 2.6× enlargement. (P) Double-immunofluorescence staining of acini from *RbpjKO;R26R* mice for amylase and β-galactosidase at P3. (Q) PCR analysis of DNA from microdissected acinar cells of *RbpjKO* (lane 1) and *Rbpj^{+/-}* (lane 2) pancreata. Schematic maps of the floxed *Rbpj* locus before and after Cre recombination are shown. The position and polarity of the primers used for amplification are represented by P8 and P9 (red arrowheads). Nuclei were counterstained with DAPI. Amy, amylase; ac, acinar; m, mesentery. Scale bars: 50 μm (100 μm in D,E).

less than in control embryos (Fig. 5V). Regarding the morphological appearance of the formed islets, the endocrine epithelium in *Notch1/2KO* embryos, and more prominently in *RbpjKO* embryos, had a disturbed appearance. In most of the endocrine cell formations, α cells were not organized around β cells, and the morphology of these islet-like structures appeared to be long rather than circular like in the control mice (Fig. 5P,Q,R). In adult pancreata of *Notch1/2KO* mice, however, the islets appeared normal and were indistinguishable from wild-type controls (data not shown).

Because *Ptf1a^{+/-}Cre(ex1);R26R* mice show mosaic Cre-induced recombination in the endocrine compartment (data not shown), we sought to analyze whether this mosaicism was also present in the different knockout lines. Co-staining of islets from *Rbpj^{+/-};R26R*, *Notch1/2KO;R26R* and *RbpjKO;R26R* mice with X-gal and the endocrine cell markers glucagon and insulin revealed that, in all three genetic backgrounds, some endocrine cells were not stained with X-gal, suggesting that these cells derived from epithelial cells that did not express, or only for a short time expressed, PTF1A (Fig. 5M-U, arrows). Conversely, we also found X-gal⁺ islets in all lines,

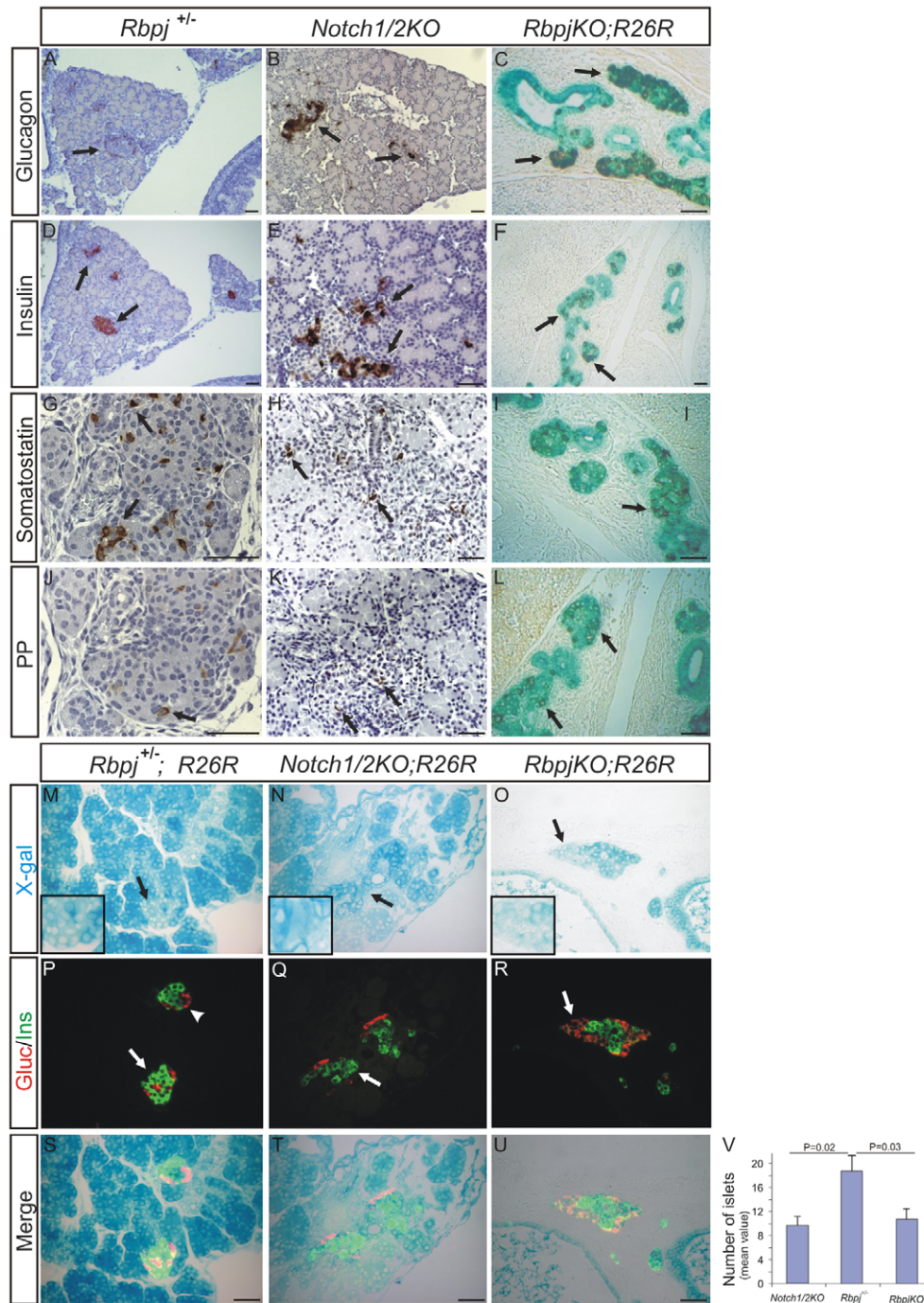


Fig. 5. Endocrine development in *RbpjKO*, *Notch1/2KO* and *Rbpj*^{+/-} pancreata. (A-L) Transverse sections from E18.5 *Rbpj*^{+/-}, *Notch1/2KO* and *RbpjKO;R26R* embryos were analyzed for the expression of endocrine markers by immunohistochemistry. *RbpjKO* pancreas was stained by X-Gal (blue) in addition to the respective endocrine genes. I, liver. (M-O) X-gal staining of sections from *Rbpj*^{+/-};R26R, *Notch1/2KO;R26R* and *RbpjKO;R26R* embryos at E18.5. Arrows mark the areas in insets (enlarged 2×). (P-R) Double-immunofluorescence staining of islets with anti-glucagon (red) and anti-insulin antibodies (green). (S-U) The merged images show co-expression of glucagon and insulin with β-galactosidase in islets of knockouts and control pancreata. (V) Histogram representing the number of islets±s.d. in pancreata of three embryos for the indicated genotype. Ins, insulin; Gluc, glucagon; PP, pancreatic polypeptide. Scale bar: 50 μm.

suggesting that incomplete deletion is not selected for in any genetic background (data not shown). Importantly, we found no difference in morphology or cellular composition between X-gal-negative and X-gal-positive islets in the different genetic backgrounds.

DISCUSSION

The regulation of organogenesis and proper cell fate determination in the pancreas has been found to involve the activation of Notch signaling. To elucidate the role of epithelially expressed Notch receptors and the specific role of the transcription factor *Rbpj* as a transducer of Notch signaling, we used a conditional gene-targeting approach to genetically inactivate either *Notch1* and *Notch2* or *Rbpj* in the pancreas.

Recently, two different mouse models for conditional genetic inactivation of *Rbpj* were described, using either transgenic *Pdx1-Cre* or *Ptf1a-Cre* knockin mice for the targeting of pancreatic progenitor cells (Fujikura et al., 2006; Fujikura et al., 2007). During early pancreatic development, both models, and our *RbpjKO* mice, revealed an essential role for *Rbpj* with premature glucagon⁺ cell development, a severe decrease in acinar cell differentiation and disturbed ductal branching in mutant mice. Differences in the phenotypical severity between these models during the early stages of organogenesis are possibly due to differences in the onset, timing and rate of Cre-induced genetic inactivation. In our *Ptf1a*^{+/-}/*Cre*^(ex1) mice, X-gal staining in the buds was observable at E10.5 in all pancreatic epithelial cells, similar

to that previously reported (Fujikura et al., 2007; Kawaguchi et al., 2002). However, even slight differences in targeting efficiency during early pancreatic organogenesis in transgenic *Pdx1-Cre* mice, and between different *Ptf1a*-knockin Cre lines, may have a large impact on the development of the respective cell compartments.

Of interest is the appearance of late exocrine cells in all models; however, phenotypical effects are notable. In our model, *RbpjKO* mice do not survive more than 4–5 days after birth, most probably as a result of the clinically apparent pancreatic insufficiency with impaired weight gain, a high content of milk in the stomach of animals and no apparent neurological phenotype. We favor this explanation over, for example, extra-pancreatic causes, as we could not detect any defects in other PTF1A-expressing organs, such as the retina or the CNS (data not shown). The reason why our *RbpjKO* mice are not able to show the same ability to develop an apparently normal adult exocrine compartment is not clear, but may possibly be explained by a more rigorous deletion of early progenitors in our mice. Nevertheless, the late appearance of acinar cells during organogenesis in our and other *Rbpj*-deficient pancreata (Fujikura et al., 2006; Fujikura et al., 2007) is surprising, and may occur through *Rbpj*-independent mechanisms involving a recently identified regulator of acinar cell development, the *Rbpj* homolog *Rbpjl* (Beres et al., 2006). These authors showed that the initiation of the acinar differentiation program by the PTF1 complex involves RBPJ κ binding to PTF1A to form the PTF1-J complex. This complex then activates RBPJL, which itself binds to PTF1A to form the PTF1-L complex. PTF1-L has been shown to be the more active complex, activating acinar genes such as amylase and elastase (Beres et al., 2006). The finding of delayed expression of acinar genes such as amylase at E18.5 in *RbpjKO* mice may be explained by two mechanisms. First, Cre activation may not be complete in a few proacinar cells, which will eventually form the exocrine pancreas. However, our results showing Cre-induced recombination of both *Rbpj* alleles in microdissected acini and in adult pancreatic tissue (Fujikura et al., 2007) do not support this hypothesis. Secondly, spontaneous activation of *Rbpjl* in precursor cells expressing PTF1A may lead to the formation of PTF1-L and, thus, to a positive-feedback loop activating the *Rbpjl* promoter. The delayed appearance and the small initial population of acinar cells would be consistent with a stochastic activation of *Rbpjl*, a hypothesis as yet unproven however.

The defective ductal branching observed in our, as well as in other, models of Notch signaling ablation may be due to early reduction of the epithelial progenitor pool, as has been suggested previously (Fujikura et al., 2006; Fujikura et al., 2007). Interestingly, the ductal cells in *RbpjKO* and *Notch1/2KO* mice expressed CK19, suggesting that the differentiation of progenitor cells into ductal cells is not inhibited by inactivated *Rbpj*-dependent Notch signaling. Future studies may help to determine the factors regulating ductal differentiation in the pancreas.

Of unclear significance is our finding of amylase positivity in dorsal duct structures of *RbpjKO* pancreata. Although we detected amylase⁺ cells within the ducts, we did not detect expression of PTF1A in these cells (data not shown); however, expression of these acinar transcription factors may be below detection limits. Other explanations include artificial staining of amylase produced by extraductal acinar cells; however, we did not observe acini in the dorsal part of the organ. Whether or not inactivated Notch signaling contributes to acinar cell fate determination from ductal cells or within ductal structures needs to be determined.

Interestingly, we found differences between *Notch1/Notch2* and *Rbpj* ablated mice regarding the severity of impaired pancreatic development. Whereas the buds of *Notch1/2KO* mice appeared smaller than those of wild-type littermates, this reduction did not reach the extent of that seen in *RbpjKO* mice. The reason for the reduced proliferation of pancreatic progenitors may be due to the requirement of Notch signals for the maintenance of actively proliferating pancreatic progenitor cells, as has recently been shown for the transcription factor *Sox9* (Seymour et al., 2007). In this regard, we also found reduced, but not completely abolished, expression of HES1 in *Notch1/2KO* and *RbpjKO* mice, as has been noted by others (Fujikura et al., 2006; Fujikura et al., 2007), possibly as a result of the expression of factors such as *Sox9*, which is necessary for the maintenance of HES1 expression. Studies with ectopic overexpression of Notch1 showed the prevention of exocrine and endocrine differentiation of pancreatic progenitor cells, leaving them in an undifferentiated state (Esni et al., 2004; Hald et al., 2003; Murtaugh et al., 2003). Despite technical issues, such as the transgenic expression and potentially non-physiological Notch1 levels, these results, as well as the aforementioned studies, point to a role for Notch in the regulation of pancreatic progenitor cells, with one of the main conclusions being a premature endocrine switch caused by insufficient Notch signaling. Interestingly however, we found such a switch in *RbpjKO* but not *Notch1/2KO* mice, possibly indicating the requirement of *Rbpj* but not *Notch1* or *Notch2* for the regulation of premature endocrine differentiation. However, we cannot rule out inefficient early Cre-induced inactivation of *Notch1* and *Notch2*. While we could determine successful recombination of both *Notch1* and *Notch2* alleles at E12.5 by PCR of microdissected epithelial cell, incomplete earlier inactivation of both Notch genes might indeed be responsible for the lack of effect in *Notch1/2KO* mice. The modest phenotype of *Notch1/2KO* mice was unexpected and is in contrast to the skin, where genetic inactivation of *Rbpj* and *Notch1/Notch2* leads to similar phenotypes (Schouwey et al., 2006). While early reports using mice null for Notch signaling family members, such as *Rbpj*, *Dll1* or *Hes1*, showed impaired growth and branching defects (Apelqvist et al., 1999; Jensen et al., 2000), differences between null mice and conditional genetic targeting approaches, such as the inactivation of targeted genes before pancreatic development is started and the additional targeting of extra-pancreatic cells in null mice, has a strong impact on the observable phenotype.

The different impact of pancreatic *Notch1/Notch2* and *Rbpj* inactivation in our study strongly suggests a Notch-independent role of *Rbpj* in pancreatic organogenesis. The near complete absence of acinar cells until late gestation suggests that RBPJ κ is required for the formation of the acinar lineage. Recent studies have shown that RBPJ κ is the binding partner of PTF1A for formation of the early PTF1-J complex (Beres et al., 2006; Masui et al., 2007; Obata et al., 2001). Our results are in line with a Notch-independent role of RBPJ κ as an obligate partner of PTF1A to form a functional PTF1 complex, a pivotal event during early pancreatic development. Thus, RBPJ κ in *Notch1/2KO* mice might still function as PTF1A-binding partner independently of its transducer role in the Notch signaling pathway.

As expected from previous reports (Apelqvist et al., 1999; Jensen et al., 2000), *RbpjKO* mice had earlier α cells underscoring the relevance of Notch signaling for the inhibition of premature differentiation of progenitor cells into early α cells. Our finding of less NGN3⁺ cells in *RbpjKO* mice is similar to the results by Fujikura and colleagues (Fujikura et al., 2006; Fujikura et al., 2007), and suggests that these endocrine progenitor cells are also

compromised and forced into premature differentiation by *Rbpj* deficiency. Notably, *Notch1/2KO* mice revealed no significant decrease in NGN3⁺ cells and several mechanisms may account for this finding. First, RBPJ κ might be activated independently and might lead to the activation of target genes; second, the four *Notch1* and *Notch2* alleles might not be inactivated in a timely manner to preserve the progenitor pool; or third, the transition of the repressor into an activator state of RBPJ κ may be, at least partially, Notch independent. Despite the premature differentiation of pancreatic progenitors in *Rbpj*-deficient mice, we found that all endocrine lineages develop in *RbpjKO* and *Notch1/2KO* mice, consistent with the hypothesis of a dispensable role of Notch signaling in late pancreatic development. However, we found fewer islets in both knockout lines, which, more prominently in *RbpjKO* mice, had a partially disturbed composition. One explanation for the development of endocrine cells despite the genetic inactivation of Notch signaling is the later expression of Cre recombinase in *Ptf1a^{+/Cre(ex1)}* compared with in *Pdx1-Cre* mice at E10.5. However, development of the endocrine compartment and islet formation does not occur before E13.5, a time point at which *Rbpj* and both Notch genes are inactivated. Our finding of X-gal⁺ islets composed of all endocrine lineages at E18.5 in both knockout lines is evidence for a non-essential role of Notch signaling in promoting endocrine cell fate determination and differentiation, whereas the lower amount of islets and the somewhat disturbed islet morphology, especially in *RbpjKO* mice, may be an at least partial result of the severe branching defect in these mice.

In conclusion, we demonstrate an essential role of *Rbpj*, but not of *Notch1* and *Notch2*, in pancreatic organogenesis. Using a concomitant approach of Notch signaling inactivation, we show that the epithelially expressed Notch receptors 1 and 2 are not essential for pancreatic development, whereas lack of *Rbpj* leads to premature differentiation of pancreatic progenitors and a decrease in endocrine progenitor cells. During late pancreatic development, however, differentiated exocrine and endocrine lineages mature in both knockout lines. Although *Rbpj* seems to be an important regulator of the early pancreatic progenitor pool, our findings strengthen the hypothesis of as yet unknown and potentially *Rbpj*-independent mechanisms regulating the cell fate of adult pancreatic cell lineages. As we can show successful inactivation of *Notch1* and *Notch2* alleles at E12.5, this finding strongly suggests that these receptors, but not *Rbpj*, are dispensable for exocrine and endocrine development. Thus, at least in the pancreas, a Notch-independent role of *Rbpj* during development seems to be a likely mechanism.

We are grateful to Jack Favor, Axel Walch and Andreas Voss for help with laser capture microscopy. We also thank Raymond J. MacDonald and Saadettin Sel for helpful discussions, and Christopher V. Wright and Tetsuo Sudo for their generous gift of PDX1 and HES1 antibodies, respectively. The CK19 antibody developed by Rolf Kemler and the Neurogenin antibody developed by O. D. Madsen were obtained from the Developmental Studies Hybridoma Bank, maintained by the University of Iowa. This work was supported in part by grants from the Deutsche Forschungsgemeinschaft to R.M.S. (SFB 4456 and SFB576), U.Z.-S. and L.S. (STR-461/3-2).

References

- Apelqvist, A., Li, H., Sommer, L., Beatus, P., Anderson, D. J., Honjo, T., Hrabe de Angelis, M., Lendahl, U. and Edlund, H. (1999). Notch signalling controls pancreatic cell differentiation. *Nature* **400**, 877-881.
- Beres, T. M., Masui, T., Swift, G. H., Shi, L., Henke, R. M. and MacDonald, R. J. (2006). PTF1 is an organ-specific and Notch-independent basic helix-loop-helix complex containing the mammalian Suppressor of Hairless (RBP-J) or its paralogue, RBP-L. *Mol. Cell. Biol.* **26**, 117-130.
- Ensi, F., Ghosh, B., Biankin, A. V., Lin, J. W., Albert, M. A., Yu, X., MacDonald, R. J., Civin, C. I., Real, F. X., Pack, M. A. et al. (2004). Notch inhibits Ptf1 function and acinar cell differentiation in developing mouse and zebrafish pancreas. *Development* **131**, 4213-4224.
- Fujikura, J., Hosoda, K., Iwakura, H., Tomita, T., Noguchi, M., Masuzaki, H., Tanigaki, K., Yabe, D., Honjo, T. and Nakao, K. (2006). Notch/Rbp-j signaling prevents premature endocrine and ductal cell differentiation in the pancreas. *Cell Metab.* **3**, 59-65.
- Fujikura, J., Hosoda, K., Kawaguchi, Y., Noguchi, M., Iwakura, H., Odori, S., Mori, E., Tomita, T., Hirata, M., Ebihara, K. et al. (2007). Rbp-j regulates expansion of pancreatic epithelial cells and their differentiation into exocrine cells during mouse development. *Dev. Dyn.* **236**, 2779-2791.
- Hald, J., Hjorth, J. P., German, M. S., Madsen, O. D., Serup, P. and Jensen, J. (2003). Activated Notch1 prevents differentiation of pancreatic acinar cells and attenuate endocrine development. *Dev. Biol.* **260**, 426-437.
- Jensen, J., Pedersen, E. E., Galante, P., Hald, J., Heller, R. S., Ishibashi, M., Kageyama, R., Guillemot, F., Serup, P. and Madsen, O. D. (2000). Control of endodermal endocrine development by Hes-1. *Nat. Genet.* **24**, 36-44.
- Kawaguchi, Y., Cooper, B., Gannon, M., Ray, M., MacDonald, R. J. and Wright, C. V. (2002). The role of the transcriptional regulator Ptf1a in converting intestinal to pancreatic progenitors. *Nat. Genet.* **32**, 128-134.
- Lammert, E., Brown, J. and Melton, D. A. (2000). Notch gene expression during pancreatic organogenesis. *Mech. Dev.* **94**, 199-203.
- Masui, T., Long, Q., Beres, T. M., Magnuson, M. A. and MacDonald, R. J. (2007). Early pancreatic development requires the vertebrate Suppressor of Hairless (RBPJ) in the PTF1 bHLH complex. *Genes Dev.* **21**, 2629-2643.
- Murtaugh, L. C., Stanger, B. Z., Kwan, K. M. and Melton, D. A. (2003). Notch signaling controls multiple steps of pancreatic differentiation. *Proc. Natl. Acad. Sci. USA* **100**, 14920-14925.
- Nakhai, H., Sel, S., Favor, J., Mendoza-Torres, L., Paulsen, F., Duncker, G. I. and Schmid, R. M. (2007). Ptf1a is essential for the differentiation of GABAergic and glycinergic amacrine cells and horizontal cells in the mouse retina. *Development* **134**, 1151-1160.
- Obata, J., Yano, M., Mimura, H., Goto, T., Nakayama, R., Mibu, Y., Oka, C. and Kawauchi, M. (2001). p48 subunit of mouse PTF1 binds to RBP-Jkappa/CBF-1, the intracellular mediator of Notch signalling, and is expressed in the neural tube of early stage embryos. *Genes Cells* **6**, 345-360.
- Radtke, F., Wilson, A., Stark, G., Bauer, M., van Meerwijk, J., MacDonald, H. R. and Aguet, M. (1999). Deficient T cell fate specification in mice with an induced inactivation of Notch1. *Immunity* **10**, 547-558.
- Schouwey, K., Delmas, V., Larue, L., Zimmer-Strobl, U., Strobl, L. J., Radtke, F. and Beermann, F. (2006). Notch1 and Notch2 receptors influence progressive hair graying in a dose-dependent manner. *Dev. Dyn.* **236**, 282-289.
- Seymour, P. A., Freude, K. K., Tran, M. N., Mayes, E. E., Jensen, J., Kist, R., Scherer, G. and Sander, M. (2007). SOX9 is required for maintenance of the pancreatic progenitor cell pool. *Proc. Natl. Acad. Sci. USA* **104**, 1865-1870.
- Siveke, J. T., Einwachter, H., Sipos, B., Lubeseder-Martellato, C., Kloppel, G. and Schmid, R. M. (2007). Concomitant pancreatic activation of Kras(G12D) and Tgfa results in cystic papillary neoplasms reminiscent of human IPMN. *Cancer Cell* **12**, 266-279.
- Siveke, J. T., Lubeseder-Martellato, C., Lee, M., Mazur, P. K., Nakhai, H., Radtke, F. and Schmid, R. M. (2008). Notch signaling is required for exocrine regeneration after acute pancreatitis. *Gastroenterology* **134**, 544-555.
- Soriano, P. (1999). Generalized lacZ expression with the ROSA26 Cre reporter strain. *Nat. Genet.* **21**, 70-71.
- Tanigaki, K., Han, H., Yamamoto, N., Tashiro, K., Ikegawa, M., Kuroda, K., Suzuki, A., Nakano, T. and Honjo, T. (2002). Notch-RBP-J signaling is involved in cell fate determination of marginal zone B cells. *Nat. Immunol.* **3**, 443-450.